Bulletin of Earthquake Engineering
https://doi.org/10.1007/s10518-021-01204-y

ORIGINAL ARTICLE

Seismic behavior of innovative hybrid CLT-steel shear wall for mid-rise buildings

Tulio Carrero[1,2] · Jairo Montaño[2] · Sebastián Berwart[2] · Hernán Santa María[1,2] · Pablo Guindos[1,2]

Received: 12 February 2021 / Accepted: 10 August 2021

Abstract

This paper examines the seismic behavior of CLT-steel hybrid walls at 6- and 10-story heights to increase seismic force resistance compared to conventional wooden walls. The ultra-strong shear walls proposed in this paper are called Framing Panel Shear Walls (FPSW), which are based on a robust articulated steel frame braced with CLT board panels and steel tendons. Timber structures are well-known for their ecological benefits, as well as their excellent seismic performance, mainly due to the high strength-to-weight ratio compared to steel and concrete ones, flexibility, and redundancy. However, in order to meet the requirements regarding the maximum inter-story drifts prescribed in seismic design codes, a challenging engineering problem emerges, because sufficiently resistant, rigid and ductile connections and lateral assemblies are not available for timber to meet both the technical and economical restrictions. Therefore, it is necessary to develop strong and cost-effective timber-based lateral systems, in order to become a real alternative to mid- and high-rises, especially in seismic countries. In this investigation, the dynamic response of cross-laminated timber (CLT) combined with hollow steel profiles has been investigated in shear wall configuration. After experimental work, research was also carried out into numerical modelling for simulating the cyclic behavior of a hybrid FPSW wall and the spectral modal analysis of buildings of 6- and a 10-stories with FPSW. A FPSW shear wall can double the capacity and stiffness.

Keywords Hybrid shear wall · Connections · Cyclic test · Seismic design · Cross laminated timber · Ductility

✉ Tulio Carrero
tecarrero@uc.cl

✉ Pablo Guindos
pguindos@ing.puc.cl

Extended author information available on the last page of the article

Published online: 20 August 2021

1 Introduction

In some seismic-prone countries, such as Chile, typical wood shear wall configurations may not have enough vertical strength for mid- and high-rise timber buildings. In Chile, the structural design standard (Instituto Nacional de Normalización 2009) was developed in timber constructions for low-rise buildings. Currently, there are two predominant structural systems are used in the world for wood construction: platform frame construction using light-frame timber building (LFTB) and cross laminated timber (CLT) construction. Nowadays, mid-height timber buildings are designed using the American Wood Council (2015) standard for the USA and EN 1995-1-1:2004+A2:2014 (2014) as the European Standard. The Chilean code for seismic design of buildings, NCh433 (Instituto Nacional de Normalización 2009) defines seismic response reduction factors (R) to reduce the elastic design forces due to the capacity of the structure to dissipate energy during an earthquake. For CLT, NCh433 defines R = 2, which in practical terms implies that CLT buildings respond as an elastic material, with negligible nonlinear incursions and energy dissipation. Therefore, it is important to develop new designs with larger ductility that can have a higher R value.

Light platform wood-frame construction is currently the most used type of construction for wood buildings up to 6 stories in many countries because of its economic viability. There are other construction systems such as mass timber shear walls, glued laminated timber braced frames, and post-and-beam systems, among others. These systems generally make economic sense for the construction of buildings over seven stories high in earthquake-prone areas, especially with seismic protection systems (see Montaño et al. (2020) for supplemental damping mechanisms in wood-framed shear walls). Tables 1 and 2 summarize the results of some recent tests of shear walls for the two current wood construction systems, as well tests on hybrid walls that are representative of some new designs.

The CLT system is becoming a more popular and more effective technology for the construction of prefabricated mid-rise buildings. Examples of experimental tests on the load-bearing capacity of CLT walls are presented in Ceccotti et al. (2006) and Gavric et al. (2015). According to Dujic et al. (2006), the importance of properly taking into account the boundary conditions and the influence of the type of vertical and horizontal loading is evident from the comparison of the behavior of differently tested panels. An important finding was that the vertical joints of the walls with gravity loads showed lower deformation capacity and initial stiffness of the walls (Gavric et al. 2013) when compared to those without gravity loads. Others, such as Shahnewaz et al. (2018), studied the strength and stiffness of CLT walls subjected to lateral loads. The results showed that the strength and stiffness of CLT walls increase significantly with an increasing number of connectors that are able to take the loads. The lateral load-bearing capacity of CLT walls does not change if the area of openings is up to 30% of the total size of the wall, but with gaps of 50% the resistance decreases considerably (Dujic et al. 2015). In general, it is assumed that a timber shear wall can suffer three deformation mechanisms in series (see Fig. 1), including rigid body rotation or overturning, rigid body translation and in-plane shear deformation Casagrande et al. (2016).

The influence of the connections is of vital importance in the structural behavior of a timber building. Therefore, the essential requirement for increased ductility of CLT construction (and therefore greater value of the reduction R-factor) is the use of dissipative connectors for shear walls (Carrero et al. 2020). A number of studies have been carried out to determine the response reduction factors (Estrella et al. 2019; Amini et al. 2018; Dechent

Table 1 Summary of wood shear wall tests regarding dimensions, thickness, vertical load applied, and lateral load strength

Tested wall		Length × Height	Type	Thickness	Vertical Load	Lateral Strength
[References]	[Wall]	[mm × mm]	[–]	[mm]	[kN/m]	P_{max} [kN]
Guiñez et al. (2019)	C240-10-02	2400 × 2400	LFTB	160	0	77.5
Branco et al. (2017)	DHC	1250 × 1950	LFTB	237	0	34.26
Popovski et al. (2011)	CA-SN-00	2300 × 2300	CLT	94	0	88.47
	CA-SN-02				10	87.24
	CA-SN-03				20	91.64
	CA-RN-04				20	99.97
	CA-S2-06				20	92.61
Pozza et al. (2014)	Wall A	2950 × 2950	CLT	85	18.5	100
Hummel et al. (2016)	W-CLT-St-10	2500 × 2500	CLT + Steel base	105	10	87.3
	W-CLT-Ti-10	2500 × 2500	CLT + Timber base	105	10	63.2
Kho et al. (2018)	Wall 8	3600 × 2400	Steel moment frame + infill plywood	254	0	242

Table 2 Summary of wood shear wall tests regarding ductility, stiffness, unit load capacity, yield and ultimate displacement

Tested wall		Stiffness	Stiffness for length unit	Unit load capacity	Equivalent viscous damping	Yielding displacement	Ultimate displacement	Ductility (Δu/Δy)
[Reference]	[Wall]	Ko [kN/mm]	Ko [kN/mm/m]	νexp[kN/m]	ξ (%)	Δy [mm]	Δu [mm]	μ
Guiñez et al. (2019)	C240-10-02	2.85	1.19	32.30	10.00	22.00	89.00	4.10
Branco et al. (2017)	DHC	0.69	0.55	27.41	27.19	45.57	65.45	1.44
Popovski et al. (2011)	CA-SN-00	3.16	1.37	38.46	16.59	25.59	64.08	2.50
	CA-SN-02	4.41	1.92	37.93	14.00	17.88	66.80	3.74
	CA-SN-03	4.19	1.82	39.84	13.64	20.03	64.39	3.21
	CA-RN-04	6.28	2.73	43.46	10.15	14.29	55.24	3.87
	CA-S2-06	4.84	2.11	40.27	12.62	16.33	46.39	2.84
Pozza et al. (2014)	Wall A	4.76	1.61	33.90	10.57	17.83	90.00	4.48
Hummel et al. (2016)	W-CLT-St-10	4.40	1.76	34.92	10.30	17.80	54.00	3.03
	W-CLT-Ti-10	3.90	1.56	25.28	8.40	14.30	78.50	5.49
Kho et al. (2018)	Wall 8	6.60	1.83	67.22	–	21.20	160.00	7.60

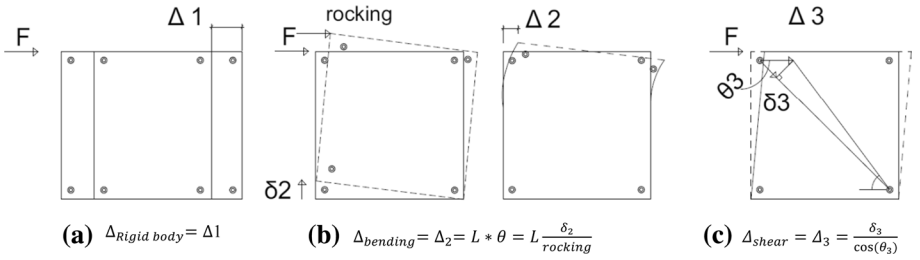

Fig. 1 **a** Lateral displacement due to rigid body; **b** Lateral displacement due to bending and overturning deformations; **c** Lateral displacement due to shear deformations

et al. 2016). Having adequate R-factors for CLT construction can lead to the design of CLT buildings with lower seismic design forces (Guindos 2020).

Solutions that include the use of post-tensioned steel cables and dissipative connections with mass timber walls have emerged recently (Priestley et al. 1999; Iqbal et al. 2015). These new technologies allow for enhanced damage-free behavior of mass timber structures in high seismic zones. These walls use energy dissipation devices such as U-Shaped Flexural Plates (UFPs) between the wall panels in coupled walls, thus providing energy dissipation. These systems avoid generating any damage and permanent deformations to the walls. Devices such as post-tensioned bars and UFPs have shown good hysteretic behavior with no evidence of loss of stiffness or problems related to the rocking effect (Priestley et al. 1999). There are a few seismic tests on post-tensioned systems in the world, for example, in the United States (Pei et al. 2019), Italy (Di Cesare et al. 2017), and New Zealand (Newcombe et al. 2010).

Some hybrid solutions aim to solve the problem of the overturning effect and, consequently, the issue of large inter-story displacements that occur during earthquakes. One such case is the use of tendons that are presented in the patent application AU2015367279 (A1) (Murray-Parkes 2016), where a connection system for walls stacked along the height of a building is described, allowing for post-tensioning the walls. This system uses CLT and a series of arrangements by means of hollow steel sections and ATS bars that have the characteristic of providing resistance to lateral forces (wind and earthquakes). The system solves the problem of rocking or overturning CLT panels but does not quantify how much it improves ductility. On the other hand, patent US9765510 (B2) (Clark Isaac Miller 2017) describes a system of structural panels for use in light construction, up to two stories. Although the described panels are hybrid, with an interior frame made of wood or metal covered by wooden plates on each side, connected by screw-type connectors, the system is limited to two stories because of the small thickness of the material, the structuring of the frame and mainly the weak connections. Also, the most crucial disadvantage is that it is quite an elaborate system; therefore, it requires the manufacturing of many special pieces that may be quite expensive if they are meant to be used in a building that is located in a high-seismicity area.

In order for timber buildings to target taller heights in a highly seismic country like Chile, it is mandatory to obtain a substantial enhancement of the lateral force-resisting system performance in terms of lateral strength, stiffness, and ductility, to decrease the cost of the structure and increase production feasibility. Hence, it is necessary to carry out further research regarding the development of elements that can provide those mechanical requirements. The hypothesis of this investigation is that hybrid frame-platform type walls are similar to typical wooden frames but combining a steel frame with CLT stiffening plates

presents better seismic behavior than conventional timber shear walls. The main objective is to develop hybrid structure resistance systems with CLT for mid-rise buildings in Chile. At this time, there is a patent pending that includes the type of wall developed in this research (Guindos et al. 2019).

1.1 Solutions for structural timber wall systems

An analysis of experimental results of eleven walls subjected to cyclic tests by several researchers is presented in this section in order to understand the mechanical properties and behavior of timber walls with different typologies in terms of ultimate load, ductility, vertical strength, stiffness, deformation characteristics, energy dissipation, damping, yield load, and yield displacement. Unit strengths and stiffness were evaluated to compare the results obtained by different authors (see Tables 1 and 2). The walls include the LFTB system, CLT walls, CLT with steel or timber frame, and plywood panels with steel frame. The walls with plywood panels and steel frame had the largest ductility and highest lateral load capacity (242 kN). The hysteretic response of CLT walls changes depending on the vertical load and the type of bottom slab (Hummel 2016). Hold-down connections in LFTB generally offer high deformation capacity but little energy dissipation, while angle brackets tolerate less deformation but offer significantly higher dissipation, Durham et al. (2001).

Test results show that CLT walls behave almost as rigid bodies during lateral load testing. Although slight shear deformations in the panels have been measured (Popovski et al. 2011), most of the panel deflections (35–83% of the total deflection (Hummel 2016) occurred as a result of the deformation of the wall in the foundation joints; this is called the rocking effect. At the same time, deformations in the panel-framing joints also made a significant contribution to the overall wall deflection. Another important fact is that it depends on the higher withdrawal resistance in CLT walls using ring nails, which exhibited higher resistance, although the ductility behaves differently (Popovski et al. 2011).

2 Hybrid shear wall proposal

2.1 Connections for hybrid walls

In the first phase of this research project, hybrid unions are defined to examine parameters related to each corresponding effect. For more information and details see Carrero et al. (2020). The connection that presented the best behavior at different damage states such as the pinching effect, stiffness degradation and strength degradation, was the CLT-Steel connection shown in Fig. 2. All the information regarding the CLT grade C24 according to the EN 1995-1-1:2004+A2:2014 (2014) and its manufacture is referred to in Carrero et al. (2020). It is essential to know that different types of specimens were manufactured for the tests, including combinations of CLT with reinforced concrete (CLT-RCwo) and with post-tensioned concrete (CLT-RCw), CLT with hollow structural steel profiles (CLT-steel) and CLT with wood, and strand rolled (LSL). The lateral resistance, ductility and high dissipation capacity of the CLT-Steel connection was better than the others tested and better than conventional wooden connections. The effect that this type of structure design has on walls would benefit on-site construction and, increase prefabrication in the manufacturing industry.

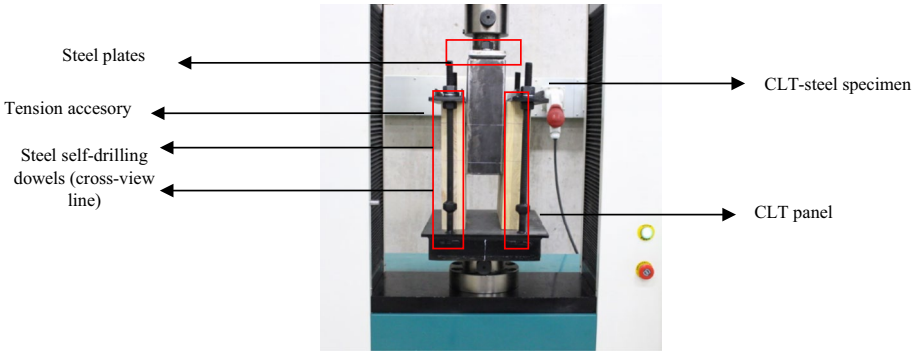

Fig. 2 Mechanical testing of the connection according to EN 12,512, including the layout for the CLT-steel connection during cyclic testing (Carrero et al. 2020)

The mechanical seismic parameters obtained from the averaged monotonic tests are summarized in Table 3; all connections are of a high-ductility class according to EN 1995-1-1:2004+A2:2014 (2014). It must noted that the CLT-LSLs connections are made with self-tapping screws, the CLT-LSLn connections with annular ring nails, and the CLT-LSLd joints with dowels. The CLT-steel connection using steel self-drilling dowels as connectors gave the highest stiffness and ductility results, Carrero et al. (2020), in comparison to the other connections tested. Full details of the hybrid CLT-steel connection design are presented in previous research (Carrero et al. 2020). Characteristic values of strength and elastic properties in N/mm^2 and density in kg/m^3 for CLT comprising timber layers derived from the properties of the timber laminations can be found in Brandner et al. (2018).

After obtaining the results of the seismic parameters of the connections, the idea is to design a wall with greater lateral load capacity. This will be done by varying the separation between the connectors and the thickness of the CLT panel (Table 4). Therefore, there is a comparison with regards to the load-carrying capacity, between 200-mm, 150-mm, 100-mm, and 50-mm self-tapping dowel spacing for each material and different panel thicknesses, among CLT with steel, concrete, and LSL (see Table 5). These results were calculated using a nonlinear model in the MCASHEW program (see Sect. 5 for more information). On the other hand, a CLT-Designer program is used to analyze the panel shear capacity for various panel thicknesses. For the admissible capacity of the CLT-steel wall with 150-mm spacing for pre-design, the lateral strength for panel shear capacity at 60 mm was verified. The hypothesis of this analysis was the consideration of ductility implemented for this type of connection, which showed good resistance behavior.

Table 3 Summary of the monotonic mechanical properties of the tested hybrid connections (Carrero et al. 2020)

Parameter	CLT-Steel	CLT-LSLs	CLT-LSLn	CLT-LSLd
K (kN/mm)	2.30	0.76	0.86	1.13
F_y (kN)	5.3	7.6	3.0	4.2
Δ_y (mm)	2.98	10.0	3.48	6.4
F_{max} (kN)	8.20	9.0	6.22	7.32
Δ_u (mm)	26.5	21.5	30	26.3
μ (unitless)	8.89	2.15	8.62	4.11

Table 4 Expected shear capacity

CLT-Designer program (KLH configuration)				2 Panel shear capacity/2.4 m
Panel thickness (mm)	Panel shear capacity/m		Layers	
60	82	kN/m	3	393.6 kN
80	106	kN/m	3	508.8 kN
100	132	kN/m	5	633.6 kN
120	166	kN/m	5	796.8 kN

Table 5 Different load-carrying capacity configurations in previous research

Load-carrying capacity					
Material	Panel	Self-tapping dowel spacing			
	Thickness (mm)	200 mm	150 mm	100 mm	50 mm
CLT-steel	60	229.04	278.72	412.27	793.71
	80	229.22	278.81	412.84	792.26
	100	229.18	278.79	413.19	791.17
	120	229.26	278.75	413.41	790.35
CLT-Rcwo	60	229.15	278.88	412.85	792.78
	80	229.29	278.76	413.4	791.08
	100	229.21	278.73	413.65	789.91
	120	229.27	278.7	413.85	789.15
CLT-LSLd	60	229.3	278.87	413.59	789.84
	80	229.35	278.79	413.97	788.22
	100	229.27	278.73	414.2	787.13
	120	229.24	278.82	414.29	786.38

2.2 Discussion of CLT-steel connection results

It is important to understand that behind the CLT-steel, there is twice the energy dissipation of the other types of connectors, see in Carrero et al. (2020). They also generate stiffer, high-strength connections compared to conventional (wood-wood) connections. In relation to details of the failure modes observed that occurred in the tests, see Carrero et al. (2020) (Fig. 3).

2.3 Development of hybrid FPSW solution

The need for a system of shear walls that allows constructing medium-height wooden buildings in highly seismic areas is evident and can be achieved by increasing the seismic response reductions factors (R) from NCh 433 (Instituto Nacional de Normalización 2009) for construction with wood; consequently, increasing the axial load capacity with respect to conventional wooden walls through the use of steel will allow to considerably reduce the number of necessary shear walls and significantly reduce construction costs.

The strong shear walls proposed in this paper (Framing CLT panel shear walls, FPSW), consist of a robust, fully articulated steel frame braced with CLT panels and

Fig. 3 Ductile failure after fatigue of the dowels in the CLT-steel connection (Carrero et al. 2020)

vertical steel tendons. The hybrid shear wall described in Fig. 4 comprises an interior frame, with hinged nodes (6), for the connection between studs-frames (3), and top–bottom beams (2), to which exterior, massive wood panels are attached on both faces (4) by means of individual CLT hybrid energy-dissipating connectors (140); the frame comprises post-tensioned self-centering tendons (4), as can be seen in Fig. 4. For more details, see the published patent of Guindos et al. (2019) in the link in the references.

Another objective of the invention (FPSW) is to provide a shear wall system that has high ductility concentrated in a high energy-dissipation effect of the system, allowing the load to be uniformly distributed along the entire perimeter of the shear wall. The final and main objective is to provide a shear wall system that allows a significant reduction of the overturning effect, avoiding the lifting and displacement of the walls, which translates into greater rigidity and reduction of the maximum value of the drift. Another aim is to provide a shear wall system that allows to reduce rehabilitation costs after the seismic event, ensuring that the integrity is not compromised when the gravitational load-bearing elements are damaged.

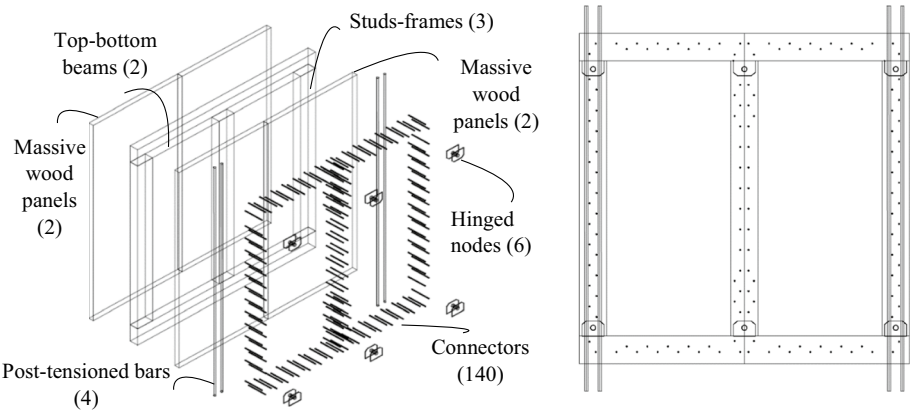

Fig. 4 Schematic isometry of Robust framing CLT, Frame-Panel Shear Wall (FPSW) based on Guindos et al. (2019)

The mechanical joints between the beams and columns are articulated node-type assemblies, consisting of a normally pivoting mechanical joint that allows an assembly with relative movement on a plane. By having this type of joint in the structure of the interior frame, the stiffness and lateral resistance of the wall are dominated by the CLT panels (see Fig. 5). The articulated joints remain in an elastic regime, limiting the displacements of the rigid body. Thus, the predominant deformation for non-slender walls is clearly shear so that the capacity and stiffness can be assumed to be proportional to the length of the wall. As the frames are made of hollow steel profiles, the mechanical connection consists of articulated nodes, preferably containing a pair of rigid steel support plates parallel to each other and crossed by a transverse pin connection. The self-tapping dowel connectors are individual elements, which are installed around the perimeter of the CLT panel. The function of the connectors is to brace the frame with respect to the seismic shear force. The connectors are the weak point of the structure, so the failure intentionally occurs there, allowing many ductilities until the ultimate failure is reached. This allows accurate prediction of stress in the components and especially in the joints so that the structural design and its experimental response can be easily predicted with great precision.

The fastening spacing in the CLT was set according to the EN 1995-1-1:2004+A2:2014 (2014). The minimum required thicknesses of members was verified to ensure ductile failure modes in all connections because this failure mode is preferred. The hybrid system should be designed by taking advantage of each material. The different results of the numerical and experimental tests might be analyzed for a final response to the study. This will indicate if we can validate the observed response with numerical modeling (MCASHEW) by Pang et al. (2007), obtaining the optimization of the system. We will also be able to know the load capacities (shear resistance) and capacities of lateral displacement (drift).

The proposed wall is based on five well-known principles. First, when bracing a hinged frame (without rotational stiffness at the connections of the frame members) with wooden boards (CLT), its stiffness and lateral resistance are governed by the board-frame joints. This implies that it is possible to significantly increase the stiffness and lateral resistance of the wall by increasing the size of the connectors and decreasing their spacing. Second, it is possible to obtain ductile failure modes (Johansen 1949, mode IV according to Instituto

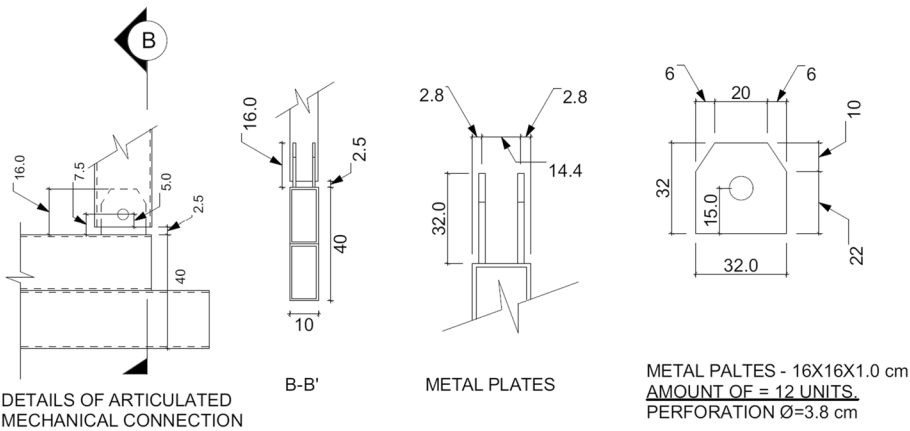

Fig. 5 Test details from the mechanical articulated connection (dimensions in millimeters)

Nacional de Normalización 2014) in slender connectors of large dimensions, as long as the minimum thickness (resistance) provided by the frame and the board is sufficient. Third, the structural redundancy and the ductility of a wooden wall increase substantially by increasing the number of connectors (reducing dowel spacing). On the other hand, it is possible to anchor a timber wall to the rigid body tipping movement (lifting or rocking) using steel cables (ATS). Thus, in addition, the wooden posts will only be applied to compression, never to tension, so that the design resistance of the same can be assumed to be much higher. Furthermore, the wooden walls that are anchored to the floor, and whose rigidity and lateral resistance are governed by the panel-frame connectors, present rigidity and lateral resistance that are linearly proportional to the length because the dominant deformation is shear. This generates a very predictable seismic response that can be calculated with simple models.

It is essential to have a mixed wood-steel shear wall in order to achieve a use of more environmentally sustainable materials. Also, it must be noted that the mixed system is much more beneficial regarding several nonstructural aspects in comparison to an only steel system, for which the fire protection is especially noteworthy. The use of steel enables the possibility of reaching a very ductile behavior between the steel-wood joint. The benefits are longer service life, zero maintenance, energy efficiency and sustainability. CLT at this time is traditionally one of the preferred materials when constructing mid-rise buildings, garnering greater support in it being the material of the future.

3 Experimental tests

This section provides a description of the test specimens and testing procedures. A discussion of the materials, construction details, instrumentation, and data acquisition system is included. The study is focused on improving the lateral behavior of shear walls in the platform frame system with hybrid shear walls applied to buildings from 6 to 10 stories high.

3.1 Test set up

The test setup is shown in Figs. 6 and 7. The test specimen consists of a wall 2400 mm long and 2400 mm high. The lower and upper hollow steel beams of the test specimen are connected to three hollow steel columns of the transverse area of each frame (200 mm × 100 mm) with a 6-mm thickness each, using a steel self-tapping dowel WS of 7 mm in diameter and 233 mm in length, alternated every 150 mm center to center (Fig. 8). The tests with no vertical load is considered a conservative way of estimating the lateral load and deformation capacity of the system, for example, tests of timber walls by Hummel et al. (2016) and Orellana et al. (2021) showed that the axial compression load in walls increases the lateral load capacity, the initial stiffness, and energy dissipation capacity.

The wood is mechanically classified as an MGP10-grade *Pinus radiata*. As can be seen in Figs. 6 and 7, the anchors used with the bars of the ATS system were not included in the configuration of this test for simplicity of implementation. The ATS bars were not included in the test because it was difficult to match the position of the ATS bars within the loading frame with the exact location of the pre-existing anchor grid (every 500 mm × 500 mm) in the lower reaction slab in the laboratory of Pontificia Universidad Católica de Chile. Instead, a steel mechanism and eight 38-mm diameter bolts were used to resist tension

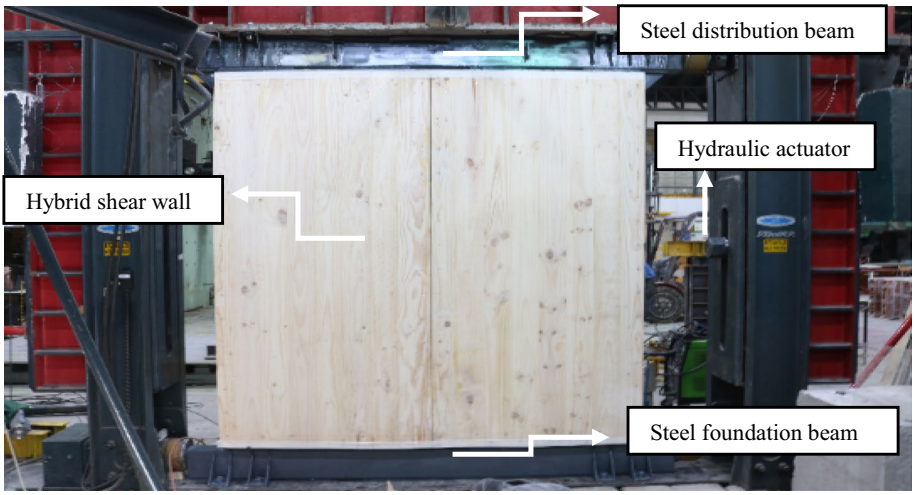

Fig. 6 FPSW wall test setup

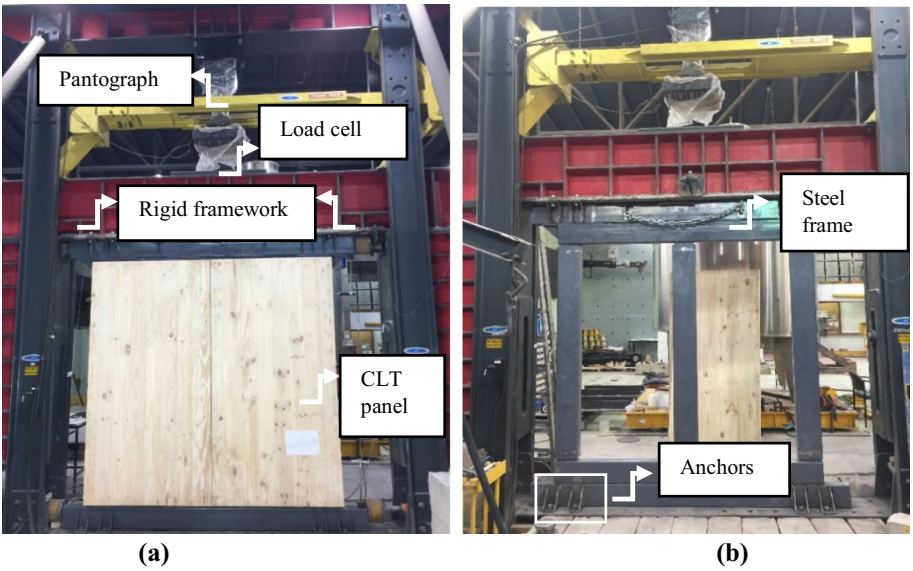

Fig. 7 Details from FPSW configuration: **a** CLT panel assembly; **b** hollow steel frame assembly

forces of 458 kN at each edge stud. Under the beams are bolts and steel teeth to allow the wall to move laterally on its plane in a free form. Vertical studs are spaced at 1200 mm.

The hydraulic actuator has a capacity of 500 kN and a travel range of ± 200 mm. It was secured between the support and the distribution beams by hinged connections, as shown in Figs. 8 and 9. The hinged connections are present to release any moment. Hydraulic jacks were placed at the foundation beam to restrict sliding of the wall obtaining only a shear deformation.

Fig. 8 Test setup procedure: **a** drilling the CLT panels; **b** pins output in drilling process; **c** mechanical articulated connections

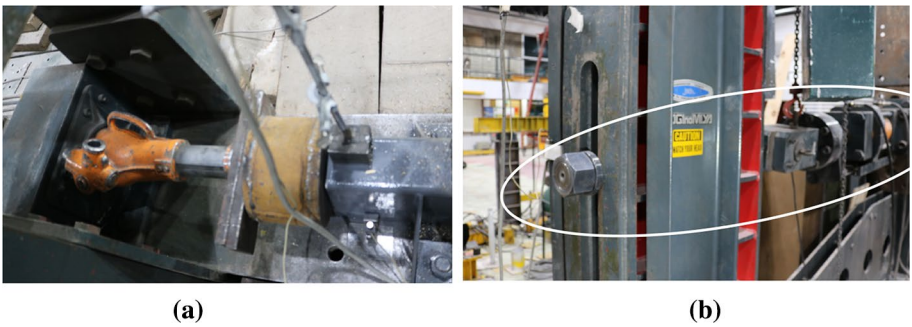

Fig. 9 Test configuration: **a** hydraulic jack to reduce displacement; **b** hydraulic actuator (500 kN)

Following the standard cyclic test (European Committee for Standardization 2013), the FPSW shear wall was set up on a total of 128 self-taping dowels (ϕ7 mm) and 6 bolted steel mechanical connections (ϕ38 mm). The timber specimens were all made of CLT produced by gluing Chilean *Pinus radiata* boards of 20 × 150 mm in cross-section and C24 grading class according to the EN 1995-1-1:2004+A2:2014 (2014) at the manufacturing plant of Forestal Tricahue Ltda., in Coronel, Chile. The gluing was performed at both of the edges and faces of the boards, casting a 3-ply laminate with a 60-mm thickness. Finally, the use of steel cables (ATS) that hold the wall axially is replaced in this case by eight bolted connections at the top and bottom of the beams from the loading frame to prevent an overturning deformation, checked on LVDT (Fig. 10).

Fig. 10 Illustration of an FPSW wall: **a** instrumentation measures behind the wall; **b** the specimen in a final loop from a reversed cyclic test on loading frame

3.2 Load protocol

The loading protocol used for the wall was the cyclic protocol used for testing (Fig. 11) according to the European Committee for Standardization (2013). The EN 12,512 method was used to perform the cyclic protocol at a speed of 0.2 mm/sec in the case of connections and 0.1 mm/sec on the walls.

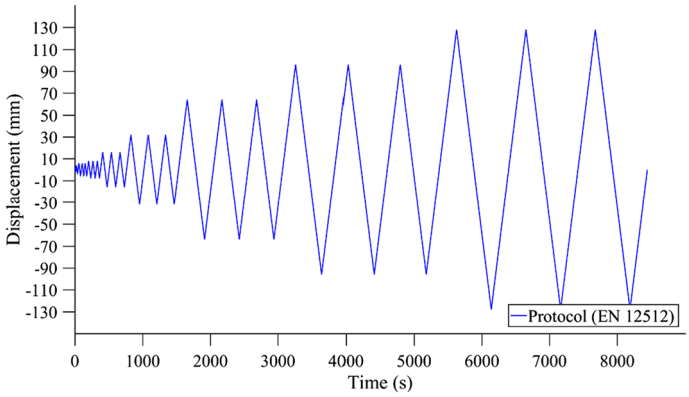

Fig. 11 A protocol according to EN 12,512 for the cyclic load test

3.3 Instrumentation

Fifteen channels of the data acquisition system (CATMAN external hardware) were used to take readings on the walls. The channel number and its corresponding measurement are given in Fig. 12. An internal linear variable differential transducer, LVDT, and the 500 kN load cell in the actuator took measures at the top of the wall.

An LVDT (channel C13) was used to measure the horizontal deflection at the top of the wall. The locations of diagonal transducers used to measure shear deformations are H and V = 250 mm. Instrumentation included vertical LVDTs located at the top and bottom of the wall to measure the overturning deformations (channels C05 through C08). In Fig. 13 we can see the test acquisition system (CATMAN) for the CLT-steel wall.

4 Test results

The results of the FPSW (CLT-steel) wall test are presented in Table 6. The strain and maximum tensile and compressive strength per cycle of the wall test are shown, as well as the secant stiffness, hysteretic dissipation energy, and equivalent viscous damping per cycle. This wall was tested in the Structural Engineering Laboratory of the Faculty of Engineering of the Pontificia Universidad Católica de Chile. The envelope for the hysteretic curve from the FPSW shear wall is presented in Fig. 14.

4.1 Experimental results per cycle

It can be noted that for load cycles up to 6, the stiffness degradation increases. On the other hand, the viscous damping increases from cycle 9. These results ultimately mean that the

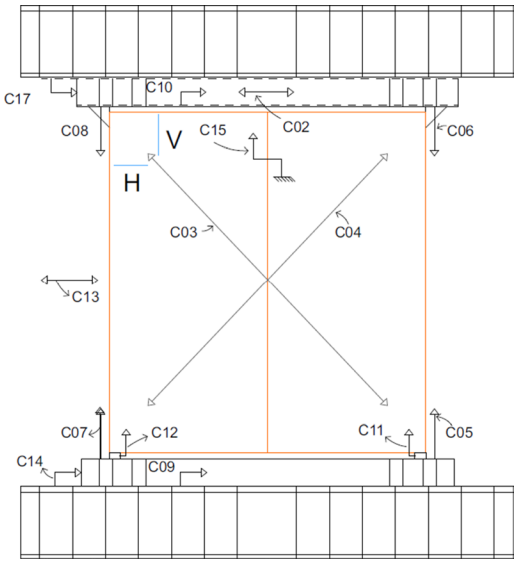

Instruments (measures):
C = HBM channel.

C15 = relative displacement measurement between CLT plates.
C11 & C12 = relative deformation measurement between CLT and lower steel sole.
C02 = global displacement of the actuator.
C03 & C04 = measurement of diagonal deformation.
C07 = left uplift bottom.
C05 = right uplift bottom.
C08 = left uplift top.
C06 = right uplift top.
C14 = bottom displacement.
C17 = top displacement.
C13 = records load (cell).
C09 = bottom relative displacement
C10 = top relative displacement

Fig. 12 Elevation-front view with LVDT locations

Fig. 13 Data acquisition equipment connected to LVDT and load cell

shear wall by itself maintains a sufficient lateral load capacity, allowing it to have high deformations in the elastic range but then reaching its load capacity drastically reduces its resistance. The graphs of Fig. 24 present further details on the degradation of stiffness and resistance. The equivalent viscous damping and dissipation energy graph are also shown.

4.2 Failure mode

The main results presented in this section are the observed failure modes of the tested wall. The FPSW wall in this study failed when the panel and frame connections either pulled out (Fig. 15c) of the framing or tore through the CLT panels (Fig. 15d). When this happened, the CLT panels were no longer effectively attached to the framing. Overall, the steel frames with the dowels (panels and frames connections) showed ductile behavior.

At a displacement of 26.83 mm, the C15 transducer (LVDT measured relative displacement between CLT plates) is corrected due to the movement of the instrumentation (Fig. 16).

4.3 Ductility evaluation

The two methods used in this investigation to calculate ductility are EN 12,512 and ASTM E2126. According to EN 12,512, it is essential to understand that the most representative parameters, according to the European Committee for Standardization (2013) that are obtained within these curves are the yielding load (F_y), yielding displacement (δ_y), maximum load (F_{max}), and maximum displacement (δ_{max}). The intersection between the red line (see details in Carrero et al. 2020) and the green line defined by the slope of the stiffness characteristic of the behavior and the slope of 1/6 of the red curve, respectively, represent the yielding point (see the graphic description in Fig. 17a). The most important result is the ductile behavior (ductility) which is nothing more than the ultimate displacement (δ_u) between the yielding displacement (δ_y).

Table 6 Wall results (FPSW)

Cycles	Δ^{+}_{max}	F^{+}_{max}	Δ^{-}_{max}	F^{-}_{max}	Average Δ_{max}	K_{sec} (kN/mm)	Dissipated hysteretic energy (ED)	Cumulative ED	$\xi_{eq}^{M}(\%)$
	(mm)	(kN)	(mm)	(kN)	(mm)		(kJ)	(kJ)	
1	2.4	13.53	− 2.03	− 10.79	2.22	5.49	0.01	0.01	8.57
2	4.03	30.30	− 4.03	− 31.48	4.03	7.67	0.06	0.07	7.26
3	6.02	52.47	− 6.25	− 56.29	6.14	8.86	0.12	0.19	5.63
4	6.02	55.21	− 6.24	− 54.92	6.13	8.98	0.08	0.27	3.6
5	6.07	55.31	− 6.01	− 50.01	6.04	8.72	0.06	0.33	3.24
6	8.1	80.51	− 8.04	− 77.18	8.07	9.77	0.21	0.54	5.28
7	8.12	80.51	− 8.06	− 75.41	8.09	9.64	0.15	0.69	3.69
8	8.02	76.69	− 8.04	− 74.53	8.03	9.42	0.13	0.82	3.34
9	16.15	145.83	− 16.26	− 146.12	16.21	9.01	1.61	2.43	10.83
10	16.72	146.51	− 16.08	− 138.76	16.4	8.70	0.95	3.38	6.47
11	16.12	129.25	− 16.05	− 134.25	16.09	8.19	0.77	4.15	5.76
12	32.24	196.53	− 32.17	− 192.02	32.21	6.03	6.54	10.69	16.64
13	32.2	179.36	− 32.76	− 180.74	32.48	5.54	4.15	14.84	11.28
14	32.09	163.67	− 32.45	− 166.22	32.27	5.11	3.51	18.35	10.5
15	64.27	220.06	− 64.24	− 200.35	64.26	3.27	18.61	36.96	21.94
16	64.09	163.97	− 64.75	− 152.40	64.42	2.46	11.37	48.33	17.76
17	64.63	135.33	− 64.47	− 128.37	64.55	2.04	9.32	57.65	17.42
18	96.2	153.38	− 96.26	− 128.08	96.23	1.46	18.99	76.64	22.32
19	96.53	93.26	− 96.35	− 83.26	96.44	0.92	11.48	88.12	21.46
20	96.31	62.17	− 96.87	− 61.00	96.59	0.64	7.96	96.08	21.29

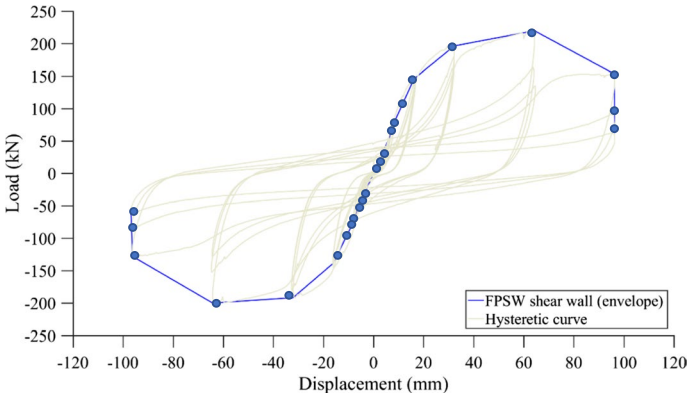

Fig. 14 FPSW envelope curve

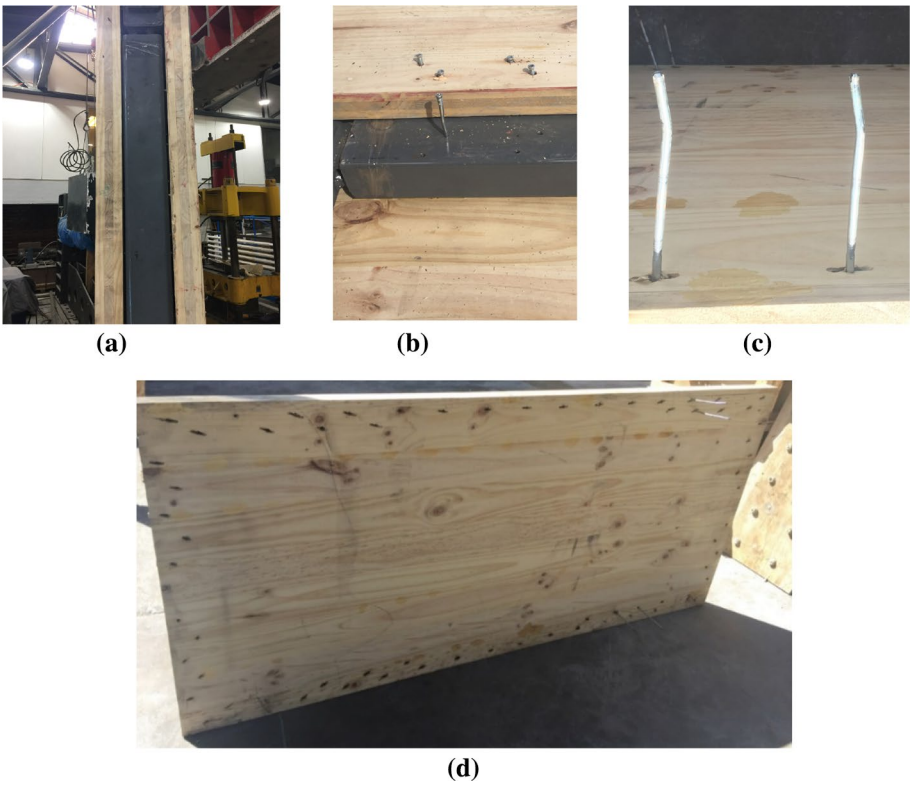

Fig. 15 The failure mode of the hybrid wall: **a** transverse view FPSW wall; **b** extraction of the dowels; **c** double plastic ball joint (failure mode f of Johansen (1949); **d** wood with poor embedment resistance and ductile behavior

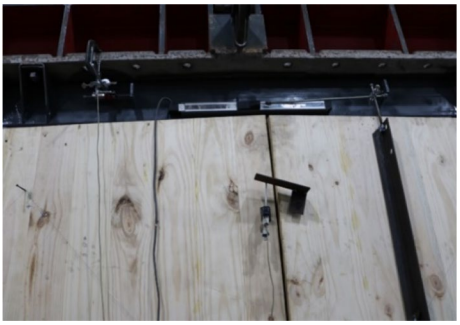

Fig. 16 Damage in middle panels of transducer C15

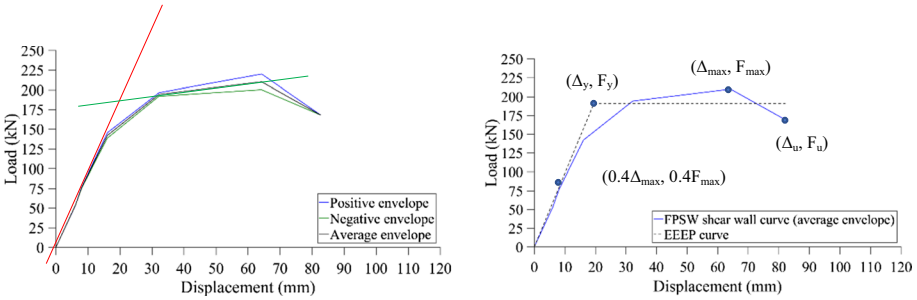

Fig. 17 **a** Average, positive and negative envelope of CLT-steel wall (FPSW) using EN 12,512 methodology; **b** Method design of CLT-steel wall according to ASTM E2126

In order to compare all the seismic parameters, this paper proposed to obtain other cyclic analyses using the guidelines in ASTM International (2019). According to the ASTM E2126 procedure, it is important to create the best representation using the envelope of the hysteresis curve given in the tests and obtaining the positive (compression) and negative (traction), understanding that the most approximate behavior is by obtaining an average. This also applies to the EN 12,512 method. The displacement Δu corresponding to the ASTM E2126 methodology is defined as 20% of the force denoted by the bilinear curve; the yield point is related to (0.4Δmax, 0.4Fmax), see Fig. 17b. The approach used is the Equivalent Energy Elastic–Plastic (EEEP). For more details, see Estrella et al. (2020), referring to the ASTM E2126 code. The parameters obtained are found in Table 7.

On the other hand, the most common method for defining equivalent viscous damping is to compare the energy dissipated in one hysteretic loop of the actual structure to an equivalent viscous system (Fig. 18). All the details regarding the calculation of the equivalent viscous damping can be found in work presented by Guiñez et al. (2019).

5 FPSW wall modeling

This section defines the important shear wall parameters that define the behavior of the specimens. As mentioned before, the critical parameters for the evaluation of shear walls are stiffness, ductility, strength, deformation characteristics, energy dissipation, damping,

Table 7 Calculation of Ductility (FPSW)

Wall	$F_{max.}$ (kN)	Δ_{max} (mm)	Δ_u (mm)	Δ_y (mm)	F_y (kN)	K_0 (kN/mm)	Dissipation energy	Ductility	$\xi_{eq}^{M}(\%)$
FPSW (CLT-steel)	*According to EN 12,512*								
	219.90	63.00	96.53	20.00	181.00	9.05	Per cycles	4.83	12.5
	According to ASTM E2126								
	219.90	63.00	82.70	20.17	190.57	9.45	Per cycles	4.10	12.5

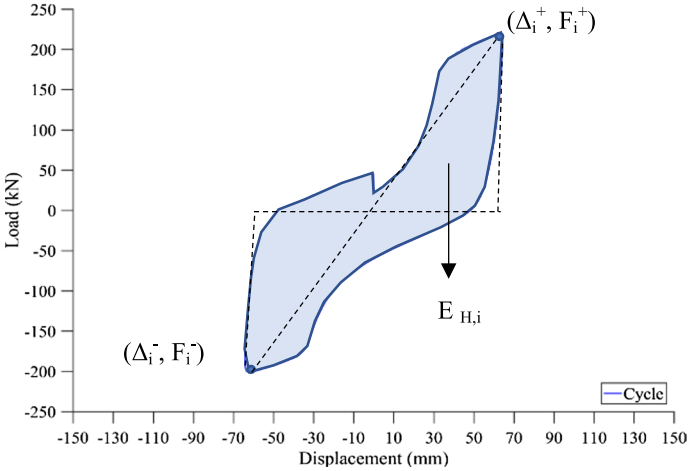

Fig. 18 Illustration of a loop for damping calculation (modified from Guíñez et al. 2019)

yield load, and yield displacement. The nonlinear model of the FPSW wall is developed in the MCASHEW software designed by Folz and Filiatrault (2001). This program is developed for conventional frame-platform walls, see Fig. 19.

For more information on the model used in this paper, see Folz and Filiatrault (2001) according to Carrero et al. (2020). In principle, there are 10 parameters shown in Fig. 19. It is essential to know that these parameters are found after obtaining the experimental curves. After that and the MSTEW model (Fig. 19), the parameters are calibrated, minimizing the cumulative energy error (CEE), for the best representation of the behavior. The results are presented in Table 8. The equation of the CEE calculation can be found in Carrero et al. (2020).

The numerical results with the MCASHEW nonlinear model indicate a maximum capacity of the first wall configuration to be tested (CLT-profile steel panels) of around 220 kN. A hysteretic load–displacement curve is plotted using the recorded data for force F and

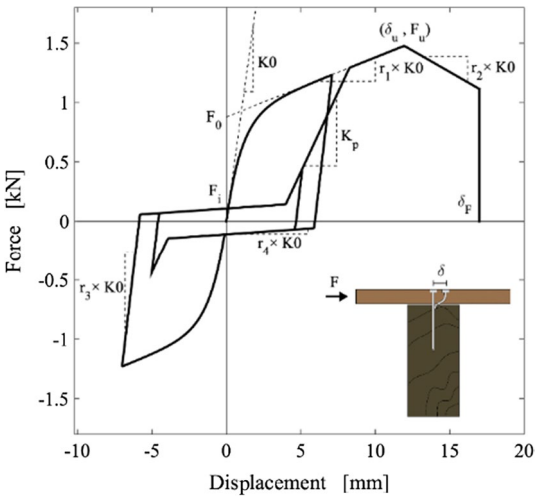

Fig. 19 Illustration of the parameters used for modelling the hysteretic response of the modified Stewart hysteretic model (MSTEW) proposed by Folz and Filiatrault (2001), based on Estrella et al. (2020)

Table 8 MSTEW hysteretic modelling parameters

Parameter	CLT-steel hybrid shear wall (FPSW)
K_0 (kN/mm)	14.3402
r_1 (unitless)	6.86E-10
r_2 (unitless)	− 0.20637
r_3 (unitless)	1.1793
r_4 (unitless)	0.02896
F_0 (kN)	217.3023
F_i(kN)	30.8793
Δ_u (mm)	57.5113
α (unitless)	1
β (unitless)	1.1607
CEE (error fit, %)	4.491

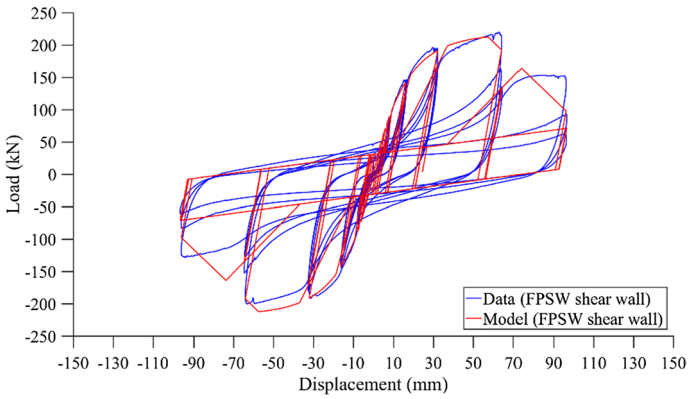

Fig. 20 Full detail of the cyclic hysteretic curve and corresponding numerical MSTEW fit of the FPSW wall (CLT-steel)

displacement Δ. The load–displacement curve is shown in Fig. 20 with full details of the cyclic hysteretic curve, and the corresponding numerical fit (nonlinear model) of the FPSW wall in the cyclic test was fully reversed (see seismic parameters in Table 8) dropped by MCASHEW.

Numerical models of the specimen were developed before testing in order to better understand the behavior of these elements when subjected to large deformations within the nonlinear range. A simplified approach was adopted to create the nonlinear model presented in this paper. Hence, some assumptions were considered in order to simplify the modeling process and minimize the data input required. In this sense, a model for platform frame walls was developed, consisting of (1) Euler–Bernoulli frame elements with three degrees of freedom per node to represent the studs and beams (hollow steel 200 × 100 × 6mm), (2) elastic plate elements with five degrees of freedom to model the CLT panels, and (3) two-node-link elements to represent the nailed CLT-steel connections and mechanical articulated joints.

The accuracy of the proposed model when predicting the load-slip response of strong wood-frame walls of different spacing ratios is verified in this section. One model was developed for each specimen for previous work in the experimental program (Carrero et al. 2020), replicating as much as possible the geometry and characteristics of each wall. The MCASHEW program develops a pushover for the representation of monotonic tests (control by displacement at 0.5 mm); for more detail in the calculation analysis, see Estrella et al. (2020). Ultimately, the important thing is that the algorithm finds 40% of the maximum capacity.

Cyclic analyses (Fig. 21) were also conducted to prove the accuracy of the model under a reversed load path. Hysteretic curves were constructed using the total lateral displacement from the EN 12,512 protocol (European Committee for Standardization 2013). The model test name implemented in this paper is FPSW240-A-B, where A refers to the dowel spacing and B to the CLT panel thickness. FPSW is the wall name and 240 is the wall length. The seismic parameters found within the modeling and testing process were ductility (μ), stiffness (K_0), and the ultimate and yielding displacements (Δ_y and Δ_u), summarized in Table 9.

Table 9 shows that ductility, stiffness, and lateral load capacity increase as the spacing of the dowels decreases. It is important to highlight that the results between the model and the experimental test for the FPSW wall capture a similarity with a tiny percentage of error. Also, the characteristic properties of nonlinear behavior, such as force, stiffness degradation, and pinching. Previous research on the concepts carried out by the authors of this paper has also demonstrated that current nonlinear numerical models are capable of capturing the hysteretic behavior of such ultra-strong connections.

Envelope curves obtained from the cyclic tests are compared to observe the effect of dowel spacing (50, 80, 100, 150 and 200 mm) and quantity (104, 128, 184, 244, 348 units) on the performance of the walls. Finally, the experimental results are compared with the estimations of strength and stiffness from ASTM International (2019).

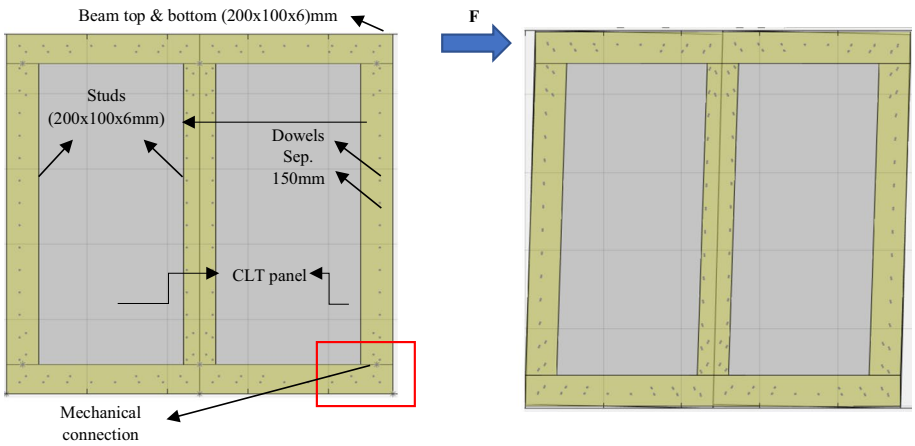

Fig. 21 MCASHEW nonlinear model prediction for the FPSW test

Table 9 Cyclic results model test from MCASHEW of CLT-steel shear wall (FPSW)

Parameters	Cyclic results model test MCASHEW)				
	FPSW240-200–60	FPSW240-150–60	FPSW240-100–60	FPSW240-80–60	FPSW240-50–60
Ductility according to EN-12512					
$\alpha =$	46	33	30	35	27
$\beta =$	0.17	0.11	0.1	0.12	0.08
$F_{max} =$	273.02	278.81	411.9	628.57	792.06
$0.40F_{max} =$	109.21	111.52	164.76	251.43	316.82
$0.10F_{max} =$	27.3	27.88	41.19	62.86	79.21
$\Delta_u =$	97.5	125	132.5	115	142
$\Delta_y =$	27.86	68.21	78.46	53.87	98.91
$F_y =$	235.71	252.38	385.96	611.11	758.33
Ductility (EN) =	3.5	1.83	1.69	2.13	1.44
Ductility according to ASTM-2126					
$0.40\Delta_{max} =$	13.57	29.74	32.82	21.74	41.76
$F_u(0.80F_{max}) =$	218.42	223.05	329.52	502.86	633.65
$\Delta_u(0.80F_{max}) =$	96.38	124.49	132.2	114	140.69
Area =	20,282	22,418	34,855	52,033	67,860
$K_0 =$	8.05	3.75	5.02	11.57	7.59
F_y (EEEP) =	251.07	243.67	362.84	587.19	736.28
$\Delta_y =$	31.2	64.98	72.28	50.77	97.05
Ductility (ASTM) =	3.09	1.92	1.83	2.25	1.45

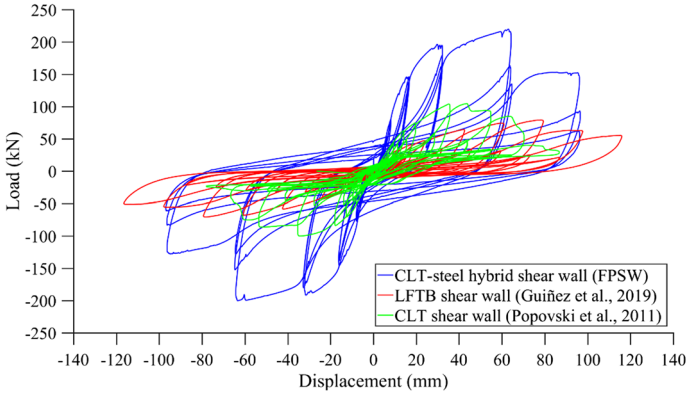

Fig. 22 Comparison of cyclic test curves from different wall tests

Fig. 23 Comparison of cyclic test curves normalized from different wall tests

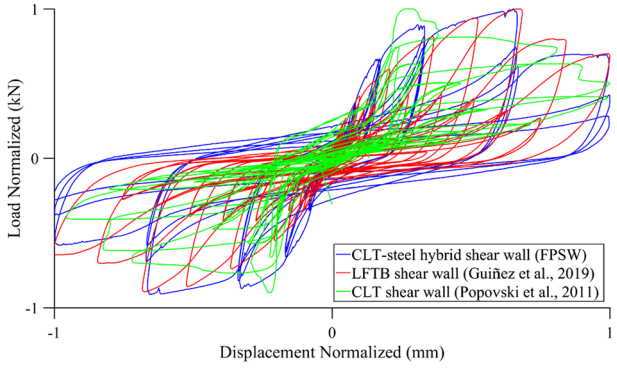

5.1 Comparison of cyclic test curves, envelope response and stiffness with CLT and LFT Walls

In Fig. 22, the hysteresis curve of the ultra-strong developed shear wall (FPSW), compared to a conventional timber LFTB and CLT wall, is presented. The main findings in this comparison of cyclic load and deformation curves is the high contribution generated by the hybrid composition of the FPSW wall, which produces better behavior under lateral loads, such as improving the stiffness in relation to the LFTB and conventional CLT wall, as can be seen clearly in the graph. The high lateral load capacity in the FPSW wall is remarkable, unlike the two walls it is compared to (LFTB and CLT), amounting to at least twice as much.

In order to be able to compare the graphs, both the load and displacement data are normalized to obtain a better version based on ductility and pinching effect. It can be seen in Fig. 23 that in the red curve (Guiñez et al. 2019) and the blue curve (FPSW), a similar ductility is appreciated, and the pinching effect is shortened in relation to the wall of the green line (Popovski et al. 2011) showing its high pinching effect.

Once the wall was analyzed, comparative graphs were made in order to evaluate the differences between the different wooden structures' configurations in contrast with

the FPSW test. For example, comparing walls that had the LFTB system (Guíñez et al. 2019) with nails (ϕ3 × 70 mm) every 100 mm versus the CLT wall (Popovski et al. 2011) with 10d annular ring nails per angle bracket in contrast to the FPSW configuration (see a hysteretic envelope from Fig. 24a). There it also evaluated what happens with dissipated energy, stiffness, and strength degradation per cycle.

5.1.1 Comparison of energy dissipation

It is essential to know the relationship (CEE) between the experimental models and the calibration of the MSTEW program in order to find the error percentages in which the CLT (Popovski et al. 2011), LFTB (Guíñez et al. 2019), and FPSW models in shear wall configurations are found. This represents a comparison parameter for energy dissipation, as illustrated in Fig. 25. In the case of shear wall testing, the primary source of energy dissipation comes from the friction of the fastener with the sheathing and framing (CLT panels and hollow steel profile).

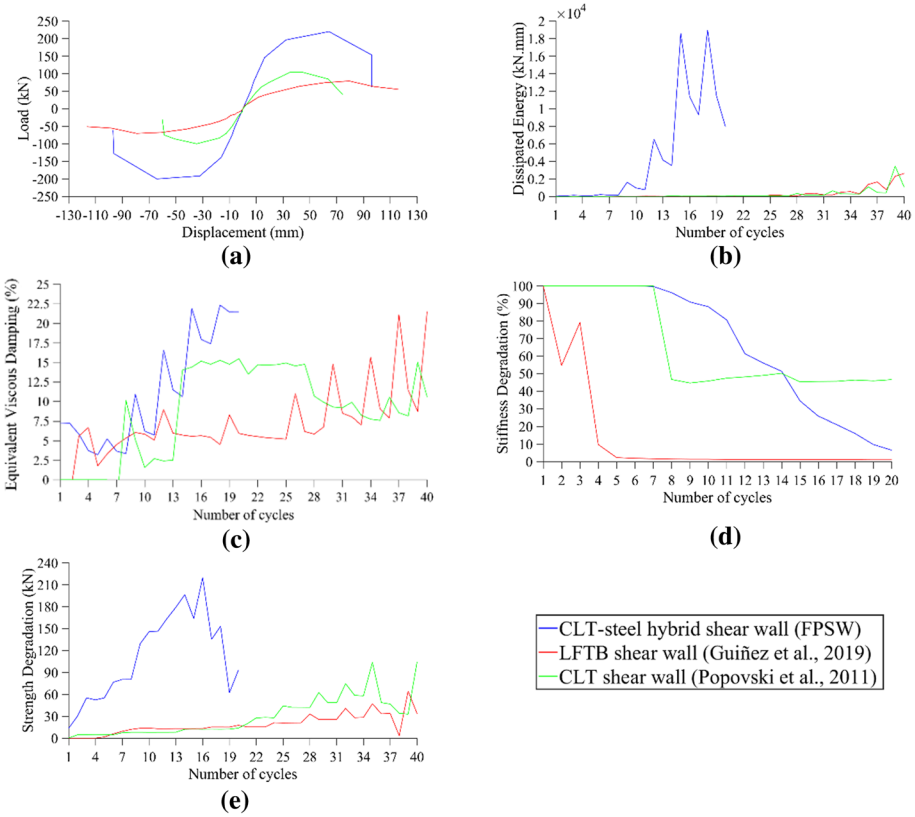

Fig. 24 Comparison of the cyclic performance of the shear walls compared including the innovation CLT-steel wall. **a** hysteresis envelopes; **b** energy dissipation per cycle; **c** equivalent viscous damping per cycle; **d** stiffness degradation per cycle; **e** strength degradation per cycle

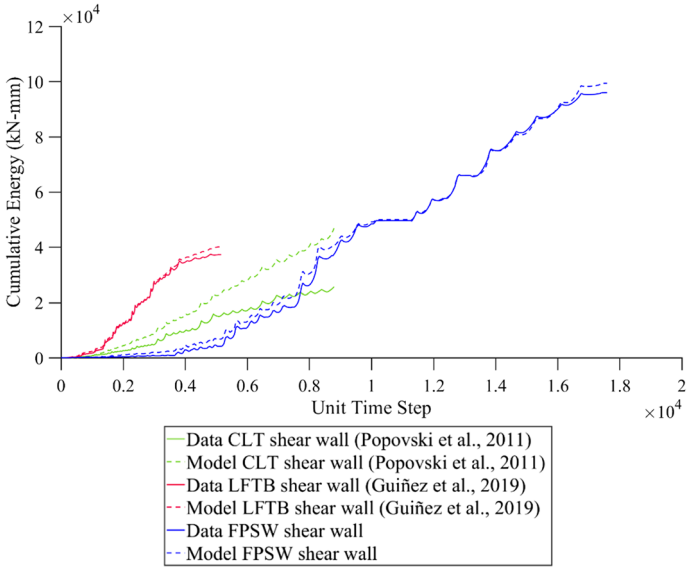

Fig. 25 Comparison of the cyclic performance of the shear walls' cumulative energy dissipation

The result indicates the high similarity between the experimental and numerical model for the cases presented, especially in the FPSW wall, the type of hybrid CLT-steel shear wall, as the error (CEE) is approximately 4.5%.

6 Building modeling

6.1 Design procedure of buildings with 6 and 10 stories

The design procedure will be for four structural systems of wooden buildings such as LFTB and FPSW for six and ten floors. The idea is to define and compare the seismic design parameters associated with FPSW and LFTB buildings. The Chilean seismic code NCh 433 will be taken into account. The buildings were designed using the Chilean Seismic Design Standard (Instituto Nacional de Normalización 2009) and the CIM methodology implemented by the Centro de Innovación en Madera (CIM) and Pontificia Universidad Católica de Chile (PUC). The maximum allowable resistance of platform frame walls was considered 0.017 kN/mm. The allowable resistance of FPSW walls is 0.046 kN/mm. For construction purposes, a 100 × 200 mm hollow steel section can fit two 1 ¾" bars.

This configuration has an effective area equal to that of a bar with a diameter of 2 ½", despite the fact that constructively we would have to put two 1 ¾" bars. The shear stiffness of the tested FPSW walls is 10 kN/mm, corresponding to the wall with self-tapping dowels every 150 mm. These values will be used to evaluate whether it is feasible to obtain six-story buildings with a lesser number of walls and whether it will be possible to reach ten floors.

The methodology to design the 6- and 10-story buildings consists of a spectral modal matrix analysis according to what is specified in (Instituto Nacional de Normalización 2009). Until now, the only reference to develop a matrix analysis for platform frame

buildings is presented by Rossi, who proposes the formulation to obtain the flexibility matrix. For the developed methodology, it generated a modification of the Rossi Flexibility Matrix formulation. In the first place, the accumulated rotation was eliminated due to the fact that this was thought to provide excessive and unrealistic displacements because, in practice, the walls cannot overturn independently on the same axis. The expression that allows obtaining the stiffness matrix of a wall in height is shown in Eq. 1.

$$\widetilde{U}_{j,,\xi} = \sum_{r=1}^{\min(j,\xi)} \frac{1}{K_{F,r}} + \frac{1}{K_{C,r}} + \frac{\left(z_\xi - z_{r-1}\right)\left(z_r - z_{r-1}\right)}{b^2 * K_{Anclaje,r}} \tag{1}$$

The above flexibility matrix is used to obtain the displacements of the building once the modal forces have been applied and accepted. Unlike Rossi, for the calculations of this paper, it is assumed that the anchors are always active, and it does not carry out a reduction in displacements due to gravitational loads. This is done with the aim of compensating for the effect of removing the accumulated turn since if this is not considered, much smaller displacements would be obtained. To obtain the fundamental period, since the Rossi methodology provided very long periods, the use of a stiffness matrix that considers the anchors not to be active was considered adequate. This is because when the building is at rest, it does not want to overturn and therefore the anchors are not in tension and there is no contribution to flexibility. In practical terms, this implies that the stiffness matrix considered to obtain the periods and modes of vibrating is given in Eq. 2.

$$\widetilde{U}_{j,,\xi} = \sum_{r=1}^{\min(j,\xi)} \frac{1}{K_{F,r}} + \frac{1}{K_{C,r}} \tag{2}$$

This matrix gives us the shortest fundamental periods, which are also consistent with the fundamental periods that have been measured in buildings and are found in the literature. An interesting scientific paper to be cited that is Casagrande et al., (2016) has presented an equation suitable to describe the elastic behavior of a single storey timber shear wall.

In order to incorporate the wall tested (FPSW), it is necessary to obtain its rigidity, which must be obtained at a load of 40% of the ultimate load. The stiffness acquired was 10 kN/mm, and according to what was discussed, this includes the flexural stiffness of the frame, the shear of the CTL boards and the self-taping dowels. This implies that, for its incorporation to generate stiffness matrices, the expression to be used would be the following equations:

$$\widetilde{U}_{j,,\xi} = \sum_{r=1}^{\min(j,\xi)} \frac{1}{K_{experimental,r}} + \frac{\left(z_\xi - z_{r-1}\right)\left(z_r - z_{r-1}\right)}{b^2 * K_{Anclaje,r}} \tag{3}$$

$$\widetilde{U}_{j,,\xi} = \sum_{r=1}^{\min(j,\xi)} \frac{1}{K_{experimental,r}} \tag{4}$$

An important issue regarding stiffness is that the shear stiffness obtained by the FPSW test (10kN) is almost twice as high as the experimental stiffness of the walls (5.4kN) of Guíñez et al. (2019). It should be considered that LFTB experimental walls have a 10-cm nail spacing, while FPSW walls have self-tapping dowels spaced 15 cm. The stiffness and deformations implemented in the calculus design shown in the following equation from American Wood Council (2015) are:

$$\delta = \left(\frac{8vh^3}{EAb}\right)_{Bending} + \left(\frac{vh}{1000nG_a}\right)_{Shear} + \left(\frac{h\Delta_a}{b}\right)_{Overtuning} \tag{5}$$

where h is the wall height in mm; b is the length of the wall in mm; E is the modulus of elasticity of the stud's edge in MPa; A is the cross-sectional area of the stud's edge at one end of the wall in mm^2; ν is the shear per unit length of the wall in kN/mm; G_a is the apparent modulus of shear wall in kN/mm (see Eq. 6); Δ_a is the total vertical deformation of the anchor in mm; traction and compression are the forces P in kN. Finally, n is the number of sheathed wall faces = 2.

$$G_a = \frac{F}{\delta_{shear}}\frac{h}{nL} \rightarrow G_a = K_{shear}\frac{h}{nL} \tag{6}$$

The overturning deformation is the lateral displacement of the wall due to the lifting of the wall as a result of the tensile deformation of the anchoring system. Therefore, Δ_a is the deformation of the anchoring system under the tensile load generated by the overturning moment (see Eq. 7), and it is necessary to know the rigidity of the anchoring system to be able to estimate the deformation.

$$\Delta_a = \frac{T_{ATS}}{K_{ATS}} = \frac{Fh}{K_{ATS}b} \tag{7}$$

The rigidity of the ATS system (post-tensioned bars) is simply the axial stiffness of the bar, which is obtained as follows, where the effective area (A_e) is from ATS bars.

$$K_{ATS} = \frac{EA_e}{L} = \frac{EA_e}{\left(h_{wall} + h_{inter-story}\right)} \tag{8}$$

It is recommended to consider the effective area in tension obtained from the expression in American Institute of Steel Construction (2016):

$$A_e = 0.7854 * \left(d - \frac{0.9743}{n}\right)^2 [\text{in}^2] \tag{9}$$

where d is the nominal diameter of the bar and n is the number of threading per inch that can be found in the AISC Steel Construction Manual 2011. Then, it is possible to calculate the equivalent wall stiffness from American Wood Council (2015) as:

$$K_{eq} = \left(\frac{8h^3}{EAb^2} + \frac{h}{1000G_a b} + \frac{h^2}{b^2}\frac{1}{K_{ATS}}\right)^{-1} \tag{10}$$

6.2 Design considerations and results

The objective of using this wall system (FPSW) is to reduce the number of structural walls in the lateral resisting system and complement it with the post beam system, with the idea of generating open-plan buildings that allow opening the market for wooden buildings in the private environment, mainly with office buildings in mind. The same building plan is

used to design a LFTB building (Fig. 26a) with the CLT-steel frame wall (FPSW) system (Fig. 26b), but with a reduced density wall by plane.

In the preliminary design of the buildings with FPSW walls corresponding to the 6-story P1 building (on floor C and zone 2) and the 10-story P2 building (on floor D and zone 3) using the Chilean code (Instituto Nacional de Normalización 2009), the design results fulfill drift and shear limit requirements for modal analysis. An important observation regarding the models is that they are designed for minimal basal shear because they have a period of approximately 0.75 s. The advantage of this design is that it allows for much fewer walls (FPSW) to be used than would be in a platform frame (LFTB) building. It is important to mention that with this design, the drift limit requirement (0.002) is achieved, which is defined as the relationship between the maximum displacement obtained from each floor and the mezzanine height when applying the seismic load (see Fig. 26).

Building with the proposed walls require less wall density in comparison to a typical wood building because the shear walls are stiffer and stronger, while maintaining the ductility. One downside of this is that the redundancy of the lateral resisting system decreases. Further studies are needed to define the seismic design parameters associated to the buildings.

6.2.1 Six-story buildings

(a) Six-story LFTB building, with all walls LFTB, designed for soil type C, and zone 2 by the Chilean seismic design code (Instituto Nacional de Normalización 2009), designed with the maximum seismic coefficient. This is the most demanded 6-story building available with traditional platform frame walls. The maximum anchorage (post-tensioned bars) diameter is 34.9 mm for walls in the X direction and 28.6 mm

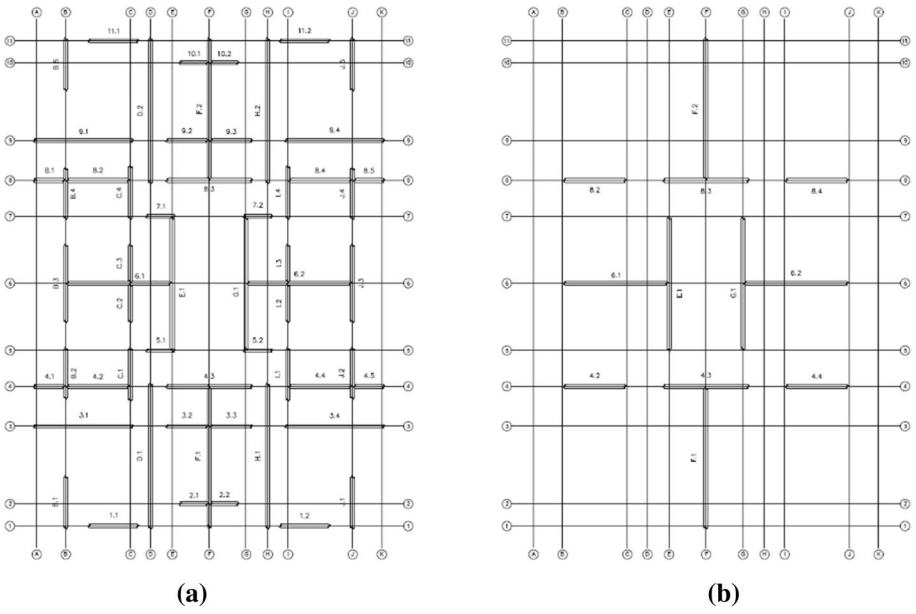

(a) **(b)**

Fig. 26 Floor plan and wall distribution of building: (**a**) normal frame-platform shear wall (LFTB) density distribution with total walls; (**b**) FPSW shear wall density distribution with some walls

for walls in the Y direction. The maximum shear demand of any of these walls is 0.017 kN/mm.

(b) Six-story FPSW building, with all walls FPSW, designed for soil C, and seismic zone 2, designed with the maximum seismic coefficient. The post-tensioned bar diameters were chosen to comply with the drift limit defined by the Chilean seismic design code (Instituto Nacional de Normalización 2009), given the experimental stiffness of the walls. The maximum anchorage diameter is 38.1 mm in direction X and 28.6 mm in direction Y. The maximum shear demand of any of the walls is 0.018 kN/mm.

(c) Six-story FPSW building with reduced number of FPSW walls, designed for soil C, and zone 2. The linear meters of FPSW walls were reduced to 63% and 73% of the original building in the X and Y directions, respectively. The building is more flexible, reducing the designed seismic coefficient. The maximum anchorage diameter is 54.0 mm in the direction X and 50.8 mm in Y direction, required to comply with the design drift limit. The maximum shear demand of any of the walls is 0.018 kN/mm. This design indicates that it is possible to reduce the number of walls by 63% and 73%, but with the need to increase the diameter of the anchors.

In conclusion, it is possible to reduce the number of walls by 63% in X and 73% in Y compared to a conventional LFTB building plan for designs of six-story buildings. On the other hand, depending on the type of soil and seismic zone, it may be necessary to anchor more than the constructive limit of two post-tensioned bars with a diameter of 1 ¾ ". Furthermore, a flexibility effect is generated that benefits the design.

This would not have been feasible for light platform frame walls (LFTB) with a maximum required resistance per wall of 0.017 kN/mm. A flexibility effect is generated that benefits the design (FPSW).

It is observed that fewer walls could be used with this system for buildings with 6 floors or less, or at least for the density of walls considered in this case.

6.2.2 Ten-story buildings

(a) Ten-story FPSW building with all FPSW walls, designed for soil C, and seismic zone 3, with the design controlled by the maximum seismic coefficient. To comply with the drift limit, diameters of 69.9 mm in the X direction and 57.2 mm in the Y direction are necessary. The maximum shear demand for any of the walls is 0.019 kN/mm.

6.3 Drift discussion

To design a 10-story building that complies with the requirements given in the Chilean code, it is necessary to increase the cross-section of the end element of the FPSW walls by at least 80%, to use diameters of threaded bars that can be placed inside the hollow steel section. On the other hand, we have to increase the area of the steel frame. In terms of shear strength, stronger walls are not required for the case of all-FPSW walls . In removing walls, stronger walls may be required; however, we will most likely consider walls with an increase in stiffness greater than 80%, which are likely to have greater strength. The drifts of the 6 and 10 story buildings met the requirements of the Chilean code (Instituto

Nacional de Normalización 2009), see Fig. 27. Figure 27 shows the calculated responses according to vibration modes for the four buildings designed.

7 Conclusions

The research in this work achieved a much stronger lateral capacity, stiffness, and ductility using a new lateral system based on a robust frame and side CLT panels along with steel tendons. The initial proof of concept, already validated in the lab, must be refined to further develop the theoretical concept achieving much more cost-effective solutions.

In general terms, a good agreement between the test and model results is observed, and the characteristic properties of nonlinear behavior, such as force and stiffness degradation and pinching, are fully captured. Previous research on the concepts carried out by the authors of this paper has also demonstrated that current nonlinear numerical models can capture the hysteretic behavior of such ultra-strong connections.

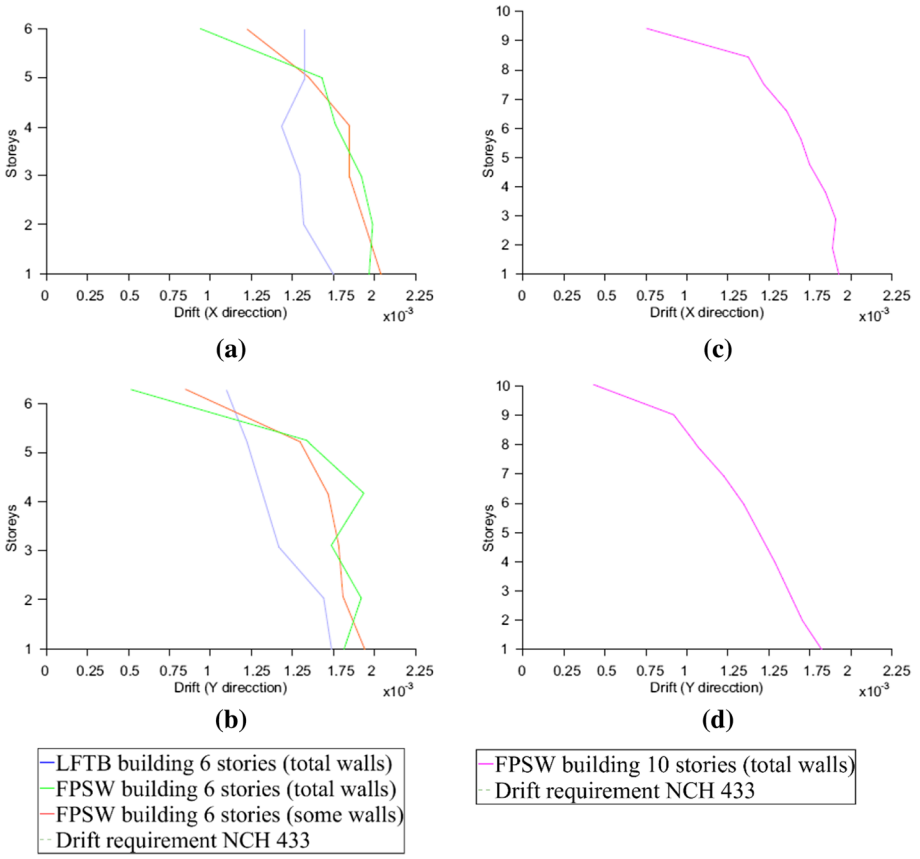

Fig. 27 Calculated response according to vibration modes **a** for building 6 storey in X direction, **b** for building 6 storey in Y direction, **c** for building 10 storey in X direction, **d** for building 10 storey in Y direction. Drifts limit requirements by Instituto Nacional de Normalización (2009)

In this investigation into ultra-strong shear walls, following and applying very innovative concepts, unprecedented stiffness, strength, and ductile shear walls are achieved in timber construction. The comparison of cyclic load-deformation curves is the high contribution generated by the hybrid composition of the FPSW wall, which produces better behavior under lateral loads, such as improving the stiffness, which can clearly be seen in the graph in relation to the LFTB and conventional CLT. The high lateral load capacity in the FPSW wall is remarkable, unlike the two walls it is compared to (LFTB and CLT) and is at least twice as high.

It is important to consider the valuable reduction in wall density by introducing the FPSW wall system in a private building plant for 6 and 10 story structures. Requirements are according to seismic codes (National Institute of Normalization 2009). The reduction varies on average 65% for 6-story buildings.

The FPSW wall system will make possible to build in seismic countries such as Chile and increase the lateral load capacity of approximately 200 kN compared to wooden structures (LFTB) of 80 kN. New studies are being developed by the research team with the same FPSW system but using different materials. This has promising results in lateral load capacity as well as cost-efficiency.

Acknowledgements This research has been funded by CONICYT Chile, FONDECYT PROJECT 11170863, and the APC was also funded by FONDECYT PROJECT 11170863. The authors thank Conicyt for the financial support, as well as the structural lab team of the Laboratory of Structural Engineering of UC and the team of the Timber Innovation Center CIM-UC. It is important to mention that an abstract was presented at the Proceedings of the 2020 Society of Wood Science and Technology International Convention on July 12–15, 2020, Slovenia. An abstract was also presented at the Proceedings of the 2021 World Conference on Timber Engineering on August 9–12, 2021, Chile.

References

American Institute of Steel Construction (2016) ANSI/AISC 360-16 Specification for structural steel buildings. AISC

American Wood Council (2015) Special design provisions for wind and seismic. ANSI/AWC SDPWS-2015, Leesburg, VA

Amini MO, van de Lindt JW, Rammer D, Pei S, Line P, Popovski M (2018) Systematic experimental investigation to support the development of seismic performance factors for cross laminated timber shear wall systems. Eng Struct 172:392–404. https://doi.org/10.1016/j.engstruct.2018.06.021

ASTM International (2019) ASTM E2126-19: Standard test methods for cyclic (reversed) load test for shear resistance of vertical elements of the lateral force resisting systems for buildings. West Conshohocken, PA, USA

Branco JM, Matos FT, Lourenço PB (2017) Experimental in-plane evaluation of light timber walls panels. Buildings 7(3):63. https://doi.org/10.3390/buildings7030063

Brandner R, Tomasi R, Moosbrugger T, Serrano E, Dietsch P (2018) Properties, testing and design of cross laminated timber. A state-of-the-art report by European Cooperation in Science and Technology Action FP1402 / WG 2

Carrero T, Montaño J, Santa-María H, Guindos P (2020) Static and dynamic performance of direct hybrid connections of cross-laminated timber with steel, concrete and laminated strand lumber composites. Lat Am J Solids Struct. https://doi.org/10.1590/1679-78256106

Casagrande D, Rossi S, Sartori T, Tomasi R (2016) Proposal of an analytical procedure and a simplified numerical model for elastic response of single-storey timber shear-walls. Constr Build Mater 102:1101–1112. https://doi.org/10.1016/j.conbuildmat.2014.12.114

Ceccotti A, Lauriola MP, Pinna M, Sandhaas C (2006) SOFIE project—cyclic tests on cross-laminated wooden panels. In: 9th World Conference Timber Engineering (WCTE), pp. 805–812. https://doi.org/10.1016/0263-8223(93)90191-R

Dechent P, Giuliano GC, Dolan JD, Silva R, Crempien J, Matamala J, Acuña G (2016) Development of a simplified design seismic-resistant method for timber multi story buildings; 2016. In: Proceedings of the WCTE 2016 World Conference on Timber Engineering, Vienna, Austria, August 22–25

Di Cesare A, Ponzo FC, Nigro D, Pampanin S, Smith T (2017) Shaking table testing of post-tensioned timber frame building with passive energy dissipation systems. Bull Earthq Eng 15(10):4475–4498
Dujic B, Aicher S, Zarnic R (2006) Testing of wooden wall panels applying realistic boundary conditions. WCTE. https://doi.org/10.1002/cphc.200500588
Dujic B, Klobcar S, Zarnić R (2015) Shear capacity of cross-laminated wooden walls. https://www.researchgate.net/publication/267692899
Durham J, Lam F, Prion HGL (2001) Seismic resistance of wood shear walls with large OSB panels. J Struct Eng 127(12):1460–1466. https://doi.org/10.1061/(ASCE)0733-9445(2001)127:12(1460)
EN 1995-1-1:2004+A2:2014 (2014) Eurocode 5: design of timber structures—Part 1-1: general-common rules and rules for buildings. Brussels, CEN, European Committee for standardization
Estrella X, Guindos P, Almazán JL (2019) Ground motions for FEMA P-695 application in subduction zones. Lat Am J Solids Struct. https://doi.org/10.1590/1679-78255848
Estrella X, Guindos P, Almazán JL, Malek S (2020) Efficient nonlinear modeling of strong wood frame shear walls for mid-rise buildings. Eng Struct. https://doi.org/10.1016/j.engstruct.2020.110670
European Committee for Standardization (2013) (CEN) EN 12512:2001/A1:2005. Timber structures–test methods—cyclic testing of joints made with mechanical fasteners. European Committee for Standardization CEN, p 123
Folz B, Filiatrault A (2001) Cyclic analysis of wood shear walls. J Struct Eng 127(4):433–441. https://doi.org/10.1061/(ASCE)0733-9445(2001)127:4(433)
Gavric I, Fragiacomo M, Popovski M, Ceccotti A (2013) Behaviour of cross-laminated timber panels under cyclic loads. RILEM Bookseries 9:689–702. https://doi.org/10.1007/978-94-007-7811-5_62
Gavric I, Fragiacomo M, Ceccotti A (2015) Cyclic behavior of CLT wall systems: experimental tests and analytical prediction models. J Struct Eng 141(11):04015034. https://doi.org/10.1061/(asce)st.1943-541x.0001246
Guindos P, Carrero T, Montaño J, Santa María H (2019) PCT/CL2019/050111. Hybrid shear wall system for construction of massive timber buildings in seismic zones. "Patent Published". https://patentscope.wipo.int/search/es/detail.jsf?docId=WO2021087630&_cid=P22-KQ1ED5-90288-1
Guindos P (2020) Conceptos Avanzados del Diseño Estructural con Madera. Parte II: CLT, Modelación Numérica, Diseño Anti-incendios y Ayudas al Cálculo. Santiago, Chile. Ediciones UC
Guíñez F, Santa María H, Almazán JL (2019) Monotonic and cyclic behaviour of wood frame shear walls for mid-height timber buildings. Eng Struct 189:100–110. https://doi.org/10.1016/j.engstruct.2019.03.043
Hummel J (2016) Displacement-based seismic design for multi-storey cross laminated timber buildings. Kassel University, Kassel. https://doi.org/10.19211/KUP9783737602891
Instituto Nacional de Normalización (2009) NCh 433. Of96: Diseño Sísmico de Edificios. Norma Chilena Oficial
Instituto Nacional de Normalización (2014) NCh 1198. Madera: construcciones en Madera—Cálculo
Iqbal A, Pampanin S, Palermo A, Buchanan AH (2015) Performance and design of LVL walls coupled with UFP dissipaters. J Earthq Eng 19(3):383–409. https://doi.org/10.1080/13632469.2014.987406
Johansen KW (1949) Theory of timber connections. Int Assoc Bridge Struct Eng 9:249–262
Kho D, Dong W, Li M, Lee C-L (2018) Cyclic behaviour of timber-steel hybrid shear walls. NZSEE Conference
Miller CI (2017) US9765510-Structural wall panels for use in light-frame construction and methods of construction employing structural wall panels
Montaño J, Maury R, Luis Almazán J, Estrella X, Guindos P (2020) Development of an amplified added stiffening and damping system for wood-frame shear walls. Lat Am J Sol Struct. https://doi.org/10.1590/1679-78256109
Murray-Parkes J (2016) AU2015367279A1: connection system—Google Patents
Newcombe MP, Pampanin S, Buchanan AH (2010) Global response of a two-storey Pres-Lam building. In: Proceedings of New Zealand society for earthquake engineering conference, Wellington, New Zealand: New Zealand Society for Earthquake Engineering
Orellana P, Santa-Maria H, Almazán J, Estrella X (2021) Cyclic behavior of wood-frame shear walls with vertical load and bending moment for mid-rise timber buildings. Eng Struct 240:112298. https://doi.org/10.1016/j.engstruct.2021.112298
Pang WC, Rosowsky DV, Pei S, Van de Lindt JW (2007) Evolutionary parameter hysteretic model for wood shear walls. J Struct Eng. https://doi.org/10.1061/ASCE0733-94452007133:81118
Pei S, van de Lindt JW, Barbosa AR, Berman JW, McDonnell E, Dolan JD, Blomgren HE, Zimmerman RB, Huang D, Wichman S (2019) Experimental seismic response of a resilient 2-story mass-timber building with post-tensioned rocking walls. J Struct Eng 145(11):04019120
Popovski M, Karacabeyli E, Ceccotti A (2011) CLT handbook-cross laminated timber. Seismic performance of cross-laminated timber buildings. FPInnovations

Pozza L, Scotta R, Trutalli D, Pinna M, Polastri A, Bertoni P (2014) Experimental and numerical analyses of new massive wooden shear-wall systems. Buildings 4(3):355–374. https://doi.org/10.3390/buildings4030355

Priestley MN, Sritharan S, Conley JR, Pampanin S (1999) Preliminary results and conclusions from the PRESSS five-story precast concrete test building. PCI J 44(6):42–67. https://doi.org/10.15554/pcij.11011999.42.67

Shahnewaz M, Tannert T, Popovski M, Alam S (2018) Strength and stiffness of CLT shear walls in platform construction. In: 18th World Conference Timber Engineering (WCTE). Seoul, Republic of Korea

Authors and Affiliations

Tulio Carrero[1,2] · Jairo Montaño[2] · Sebastián Berwart[2] · Hernán Santa María[1,2] · Pablo Guindos[1,2]

Jairo Montaño
jamontano@uc.cl

Sebastián Berwart
siberwart@uc.cl

Hernán Santa María
hsm@ing.puc.cl

[1] Department of Structural and Geotechnical Engineering, Pontificia Universidad Católica de Chile, Av. Vicuña Mackenna, 6904411 Santiago, Chile

[2] UC Center for Wood Innovation (CIM), Pontificia Universidad Católica de Chile, Av. Vicuña Mackenna, 6904411 Santiago, Chile